

AD 673974

Office of Naval Research

Contract N00014-67-A-0109-0003

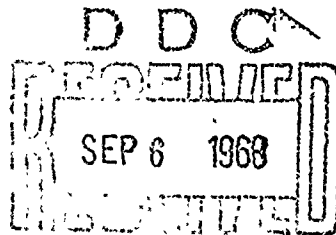
Task NR 064-496

Technical Report No. 21

THE LATERAL BUCKLING OF A STRAIGHT OR
CURVED BEAM SUBJECTED TO PURE BENDING

by

F. E. Vanslager



Department of the Aerospace and Mechanical Engineering Sciences
UNIVERSITY OF CALIFORNIA, SAN DIEGO
La Jolla, California

July 1968

Reproduced by the
CLEARINGHOUSE
for Federal Scientific & Technical
Information Springfield Va. 22151

This document is available
for public release and sale; its
distribution is unlimited.

42

Table of Contents

	<u>Page</u>
Abstract	ii
Nomenclature	iii
1. INTRODUCTION	1
2. BASIC EQUATIONS	2
3. METHOD OF SOLUTION	3
a. Curved Beam	3
b. Straight Beam	18
4. EXPERIMENTAL RESULTS	20
5. SUMMARY	31
APPENDIX	33
REFERENCES	35

THE LATERAL BUCKLING OF A STRAIGHT OR
CURVED BEAM SUBJECTED TO PURE BENDING*

by

F. E. Vanslager†

Department of the Aerospace and Mechanical Engineering Sciences
University of California, San Diego
La Jolla, California

ABSTRACT

This paper presents a new analysis of the classical problem of the lateral buckling under pure bending of a curved beam with circular axis. Although a solution to this problem, and to the corresponding straight beam problem, is well-accepted in the literature, the present analysis gives buckling moments which are significantly different than the usually accepted results. The difference arises from an application of new boundary conditions that are shown to be the only boundary conditions consistent with the equilibrium of the buckled beam under a pure bending moment. This new analysis provides generally higher bending moments. A short experimental program was performed, and the results tend to confirm the new analysis.

* The results presented in this paper were obtained in the course of research sponsored under Contract No. N00014-67-A-0109-0003 Task NR 064-496 by the Office of Naval Research, Washington, D.C.

† Research Assistant

Nomenclature

a_k, A_k	arbitrary constants
b_k, B_k	arbitrary constants
C	torsional rigidity about the centroidal axis
E	Young's modulus
I_x, I_y	second moment of the area about the x and y axes
k	an eigenvalue of eq. (3) or (23)
l	an eigenvalue of eq. (3)
L	length of a straight beam
M, \vec{M}	bending moment vector
M_x, M_y, M_s	components of the bending moment vector
n	an integer
P, P_k, P_t	axial force
R	mean radius
s	coordinate along the centroidal axis
u	displacement in the x direction
U	work of deformation
v	displacement in the y direction
V	potential energy
W_1, W_2	work of external forces
x, x'	coordinate in the radial direction
y, y'	coordinate transverse to the beam
α	beam angle

β	unit twist about the centroidal axis
γ	an angle change
δ	a length change
Δ	change in radius of curvature
ϵ	an arbitrarily small constant
κ_x, κ_y	curvature changes in the x and y directions
ν	Poisson's ratio
ρ	deformed radius of curvature
ϕ	angular displacement of the cross section

1. INTRODUCTION

This paper is concerned with the well-known problem of the lateral buckling under pure bending of a straight beam or of a curved beam with a circular axis. A sketch of a curved beam of rectangular cross section with mean radius R and opening angle α is shown in Figure 1. It is assumed that the beam is loaded by moments M acting

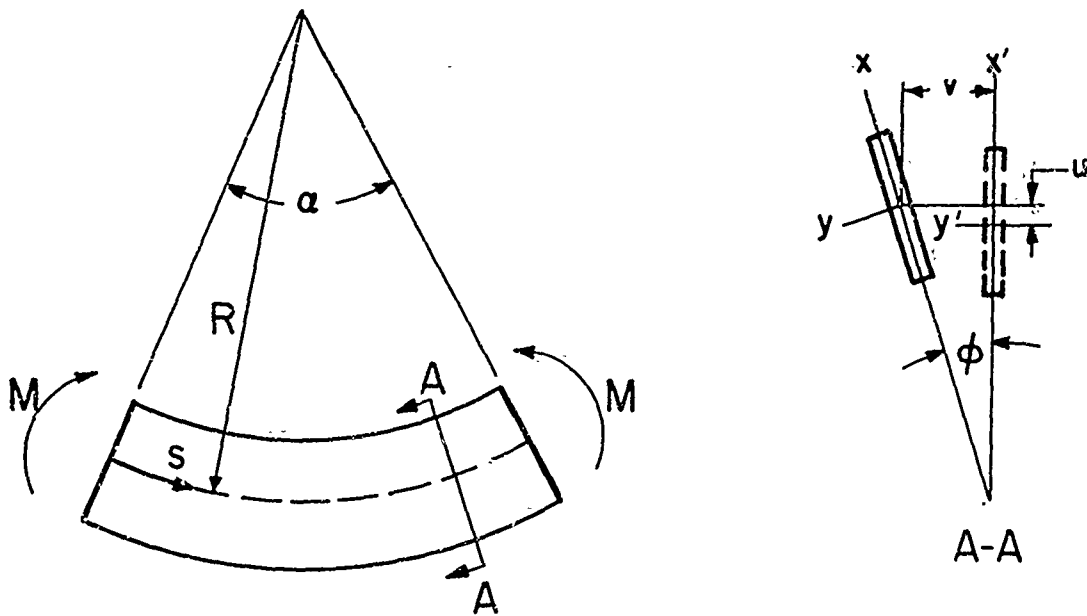


Figure 1.

at $s = 0$ and $s = \alpha R$ and is otherwise unloaded. In order to have a conservative system, it is also assumed that the direction of the applied moment vector does not change during the buckling process. When the applied moment M reaches a critical value, the planar configuration becomes unstable, and the beam begins to deform laterally. Section A-A shows the displacement of a typical cross section of the buckled

beam; the initial position is indicated by the dashed rectangle.

The classical solution to this problem, obtained by S. Timoshenko and published in Bull. Polytech. Inst. Kiev in 1910, is widely accepted, viz [1], [2]*, and, to the author's knowledge, it has never been disputed. In the first part of the present paper, a different solution is obtained for both the circularly curved beam and the straight beam. The last part of the paper describes an experimental verification of the new solutions as opposed to the classical solutions. The discrepancy between the two solutions is shown to be due to the boundary conditions prescribed on the loaded ends $s = 0$ and $s = \alpha R$. The only conditions that are consistent with the basic equations [1] are shown to be those of zero geometric constraint — i. e., "free edges", and the solution for these conditions is derived in section 3 below.

2. BASIC EQUATIONS

The linearized strain-displacement relations for the transverse curvature κ_x , the in-plane curvature change κ_y , and the unit twist β are [1], [3],

$$\kappa_x = \frac{\varphi}{R} - \frac{d^2 v}{ds^2}, \quad \kappa_y = \frac{u}{R^2} + \frac{d^2 u}{ds^2}, \quad \beta = \frac{d\varphi}{ds} + \frac{1}{R} \frac{dv}{ds} \quad (1a)$$

where u and v are linear displacement components and φ is a rotation as shown in Figure 1. The stress-strain relations are given by

$$\kappa_x = \frac{M_x}{EI_x}, \quad \kappa_y = \frac{M_y}{EI_y}, \quad \beta = \frac{M_s}{C} \quad (1b)$$

* Numbers in brackets refer to references in the List of References.

where M_x , M_y , and M_s are the components of the moment vector \vec{M} in the x , y , and s directions, I_x and I_y are the second moments of the cross section about the x and y axes, and C is the torsional rigidity about the centroidal axis. The equations of equilibrium [1] for the buckled beam loaded only by end moments M are

$$M_x(s) = M\phi \quad , \quad M_y(s) = M \quad , \quad M_s(s) = M \frac{dv}{ds} \quad (2)$$

Substitution of κ_x and β from equations (1b) and (2) into equations (1a), and elimination of v between the first and third of equations (1a) gives the classical results

$$\frac{d^2\phi}{ds^2} + k^2\phi = 0 \quad (3)$$

where

$$k^2 = \frac{1}{EI_x C} \left(M - \frac{EI_x}{R} \right) \left(M - \frac{C}{R} \right) \quad (4)$$

The general solutions of this equation can be written as

$$\phi_0 = a_0 s + b_0 \quad , \quad (5)$$

$$\phi_k = a_k \sin ks + b_k \cos ks \quad .$$

3. METHOD OF SOLUTION

a. Curved beam

The classical approach is to apply the "simply supported" boundary conditions that $\phi_k = 0$ at $s = 0$ and $s = \alpha R$, which leads to

$$\varphi_k = a_k \sin ks \text{ where } k = \frac{n\pi}{\alpha R} \text{ and } n = 0, \pm 1, \pm 2, \dots \quad (6)$$

or, alternatively, to apply the "built-in" boundary conditions that $\frac{d\varphi_k}{ds} = 0$ at $s = 0$ and $s = \alpha R$, which leads to

$$\varphi_k = b_k \cos ks \text{ where } k = \frac{n\pi}{\alpha R} \text{ and } n = 0, \pm 1, \pm 2, \dots \quad (7)$$

However, an inspection of equation (4) shows that both of these solutions lead to a finite positive buckling moment for an infinitely long beam, since equations (4), (6), and (7) show that $k \rightarrow 0$ ($M \rightarrow C/R$ or EI_x/R) as $\alpha \rightarrow \infty$. Another objection is that, as shown by equations (3) and (4), the minimum buckling moment $M = 0$ occurs when $k = \frac{1}{R}$, and corresponds to a rigid body rotation about a diameter*. Therefore, since equations (6) and (7) would give $k = \frac{1}{R}$ for $\alpha = \pi$ and $n = 1$, the buckling moment would change from a small negative value to a small positive value as the beam angle α passes through π . A plot of the negative buckling moment vs. beam angle α would, therefore, show a discontinuous jump to the next higher mode at $\alpha = \pi$. And, finally, since the rigid body rotation solution with $k = \frac{1}{R}$ should be independent of the angle α , and since equations (6) and (7) show that $k = \frac{1}{R}$ occurs only for discrete values of α , we conclude that equations (6) and (7) are probably not the correct solutions to the problem.

What, then, is wrong with this classical approach? For an

* One could equally well take $k = -\frac{1}{R}$ as the fundamental rigid body rotation but this has some notational disadvantages.

answer we must take a closer look at the statement of the problem. It is simply the question of determining the magnitude of the equal and oppositely directed end moments M , at which the beam begins to laterally deform in some unknown fashion. Equation (3) is, therefore, derived by assuming that the deformed beam is in equilibrium with an end moment M which moves with the beam, but whose direction remains fixed in space. Since no geometric boundary conditions are implied in the derivation of equation (3), the ends are essentially "free", and any solution of equation (3) is potentially a solution of the problem. In general, however, arbitrary boundary conditions will give rise to shearing forces on the boundaries which were not included in the derivation of equation (3). Therefore, additional principles must be invoked in order to determine what are the correct boundary conditions for the problem. It turns out that, since $k = \frac{1}{R}$ is a solution to the problem, it is sufficient to require that the principle of stationary potential energy be satisfied; i. e., in the vicinity of the true solution, the work of deformation must be equal to the work of the applied moment M .

In evaluating the potential energy for the beam, we will assume that I_y is very large in comparison to I_x and C . The work of deformation U will then be given by

$$U = \frac{EI_x}{2} \int_0^{\alpha R} \kappa_x^2 ds + \frac{C}{2} \int_0^{\alpha R} \beta^2 ds ,$$

or, by using equations (1) and (2),

$$U = \frac{M^2}{2EI_x} \int_0^{\alpha R} \varphi^2 ds + \frac{C}{2\left(1 - \frac{C}{MR}\right)^2} \int_0^{\alpha R} \left(\frac{d\varphi}{ds}\right)^2 ds \quad (8)$$

The work of the applied moment can be split into two parts. The first part is the work due to the "shortening" (or "lengthening") δ , which causes an angle change γ approximately given by

$$\gamma = \frac{\delta}{R} = \frac{1}{2R} \int_0^{\alpha R} \left(\frac{dv}{ds}\right)^2 ds$$

Since the applied moment stays constant during the buckling process, this part of the work of the applied moment will be simply given by $M\gamma$. By using the relationship between v and φ obtained from equations (1) and (2), the work due to the "shortening" can be written as

$$W_1 = M\gamma = \frac{C^2}{2MR\left(1 - \frac{C}{MR}\right)^2} \int_0^{\alpha R} \left(\frac{d\varphi}{ds}\right)^2 ds \quad (9)$$

The second part of the work of the applied moment comes from the "rotation" of the ends due to the apparent opening or closing of the ring. This rotation is equal to the integral along the length of the beam of the curvature changes (in the original plane) caused by the buckling. The projection of the bending curvature on the original plane contributes to this curvature change an amount

$$\kappa_x \sin \varphi \approx \kappa_x \varphi = \frac{M\varphi^2}{EI_x}$$

The last expression has been obtained from equations (1) and (2). In addition, due to the swinging of the cross section through an arc φ ,

there is a small change in curvature of amount

$$\frac{1}{R} - \frac{1}{\rho} = \frac{1}{R} - \frac{1}{R - \Delta} \approx -\frac{\Delta}{R^2} = \frac{R(\cos \phi - 1)}{R^2} \approx -\frac{\phi^2}{2R}$$

Integrating these curvature changes along the length of the beam to get the total angle change and multiplying by the applied moment M , we get that the work W_2 due to the "rotation" of the ends is given by

$$W_2 = \left(\frac{M^2}{EI_x} - \frac{M}{2R} \right) \int_0^{\alpha R} \phi^2 ds \quad (10)$$

Subtracting W_1 and W_2 from the work of deformation U , we find, after some rearrangement, that the potential energy V can be written as

$$V = -\frac{M}{2EI_x} \left(M - \frac{EI_x}{R} \right) \int_0^{\alpha R} \phi^2 ds + \frac{CM}{2 \left(M - \frac{C}{R} \right)} \int_0^{\alpha R} \left(\frac{d\phi}{ds} \right)^2 ds \quad (11)$$

Using the definition of k given by equation (4), this can also be written as

$$V = -\frac{MC}{2 \left(M - \frac{C}{R} \right)} \left[k^2 \int_0^{\alpha R} \phi^2 ds - \int_0^{\alpha R} \left(\frac{d\phi}{ds} \right)^2 ds \right] \quad (12)$$

In this form it can be readily seen that the Euler-Lagrange equation corresponding to the minimization of the potential energy V is the equilibrium equation (3). This is as it should be, indicating that the potential energy has been correctly derived.

We can now apply the principle of stationary potential energy.

We take a varied state in the form

$$\varphi^* = \varphi_k + \epsilon \varphi_l \quad (13)$$

where φ_k is the assumed "true" solution to equation (3) under the applied moment determined by k from equation (4), φ_l is the "true" solution of equation (3) with k replaced by l , and ϵ is an arbitrarily small constant. Substituting (13) into (12) and requiring that the potential energy be stationary at the true solution φ_k , we obtain

$$-\frac{2\left(M - \frac{C}{R}\right)}{MC} \frac{\partial V(\varphi^*)}{\partial \epsilon} \Big|_{\epsilon \rightarrow 0} = k^2 \int_0^{\alpha R} \varphi_k \varphi_l ds - \int_0^{\alpha R} \left(\frac{d\varphi_k}{ds}\right) \left(\frac{d\varphi_l}{ds}\right) ds = 0. \quad (14)$$

We now take another varied state in the form

$$\varphi^{**} = \varphi_l + \bar{\epsilon} \varphi_k \quad (15)$$

where now the applied moment is determined by l , and the roles of φ_k and φ_l have been reversed. Then, requiring the potential energy to be stationary at the true solution φ_l , we obtain

$$-\frac{2\left(M - \frac{C}{R}\right)}{MC} \frac{\partial V(\varphi^{**})}{\partial \bar{\epsilon}} \Big|_{\bar{\epsilon} \rightarrow 0} = l^2 \int_0^{\alpha R} \varphi_k \varphi_l ds - \int_0^{\alpha R} \left(\frac{d\varphi_k}{ds}\right) \left(\frac{d\varphi_l}{ds}\right) ds = 0. \quad (16)$$

Thus, if $k^2 \neq l^2$, we obtain from equations (14) and (16)

$$\int_0^{\alpha R} \varphi_k \varphi_l ds = 0 \quad , \quad (17)$$

$$\int_0^{\alpha R} \left(\frac{d\varphi_k}{ds}\right) \left(\frac{d\varphi_l}{ds}\right) ds = 0 \quad .$$

These orthogonality relations between the eigenvectors are analogous

to the orthogonality relations for the buckling of a straight beam under an axial force (see the Appendix). By integrating equations (17) by parts and using equation (3), one can obtain the natural homogeneous boundary conditions on the φ_k . These are

$$\left[\varphi_k \frac{d\varphi_l}{ds} \right]_0^{\alpha R} = 0 ,$$

and

$$\left[\varphi_l \frac{d\varphi_k}{ds} \right]_0^{\alpha R} = 0 .$$

(18)

The orthogonality conditions are sufficient to determine the eigenvalues k uniquely when it is remembered that the rigid body rotation solution must be an allowed solution to the problem. In order to emphasize that $k = \frac{1}{R}$ is a solution of this buckling problem, we will rewrite equations (5) in terms of odd and even parts, with this rigid body rotation solution explicitly included as follows:

$$\varphi_0 = A_0 \left(\frac{s}{R} - \frac{\alpha}{2} \right) + B_0 ,$$

$$\varphi_1 = A_1 \sin \left(\frac{s}{R} - \frac{\alpha}{2} \right) + B_1 \cos \left(\frac{s}{R} - \frac{\alpha}{2} \right) , \quad (19)$$

$$\varphi_k = A_k \sin k \left(s - \frac{\alpha R}{2} \right) + B_k \cos k \left(s - \frac{\alpha R}{2} \right) .$$

When the orthogonality conditions (17) are applied to equations (19), one obtains, after some manipulation,

$$\begin{aligned}
(A_1 A_k + B_1 B_k) \frac{\sin\left(k - \frac{1}{R}\right) \frac{\alpha R}{2}}{k - \frac{1}{R}} - (A_1 A_k - B_1 B_k) \frac{\sin\left(k + \frac{1}{R}\right) \frac{\alpha R}{2}}{k + \frac{1}{R}} &= 0, \\
(A_1 A_k + B_1 B_k) \frac{\sin\left(k - \frac{1}{R}\right) \frac{\alpha R}{2}}{k - \frac{1}{R}} + (A_1 A_k - B_1 B_k) \frac{\sin\left(k + \frac{1}{R}\right) \frac{\alpha R}{2}}{k + \frac{1}{R}} &= 0, \\
(A_l A_k + B_l B_k) \frac{\sin(k-l) \frac{\alpha R}{2}}{k-l} - (A_l A_k - B_l B_k) \frac{\sin(k+l) \frac{\alpha R}{2}}{k+l} &= 0, \\
(A_l A_k + B_l B_k) \frac{\sin(k-l) \frac{\alpha R}{2}}{k-l} + (A_l A_k - B_l B_k) \frac{\sin(k+l) \frac{\alpha R}{2}}{k+l} &= 0.
\end{aligned} \tag{20}$$

The solutions (19) that satisfy (20) and have real coefficients are of the form

$$\phi_k = A_k \left[\sin k \left(s - \frac{\alpha R}{2} \right) \pm \cos k \left(s - \frac{\alpha R}{2} \right) \right], \tag{21}$$

where the eigenvalues are given by

$$k = \frac{2n\pi}{\alpha R} + \frac{1}{R}, \quad n = 0, \pm 1, \pm 2, \pm 3, \dots \tag{22}$$

Whichever sign is used in equation (21), it must be used for all of the eigenfunctions in order for them to be mutually orthogonal. At the isolated points where α is a multiple of π , the coefficients A_k and B_k can be assigned in an arbitrary manner. However, since we are concerned here with the behavior of a real beam, these isolated points are of no particular importance.

Figure 2 shows a plot of the three lowest eigenvalues from

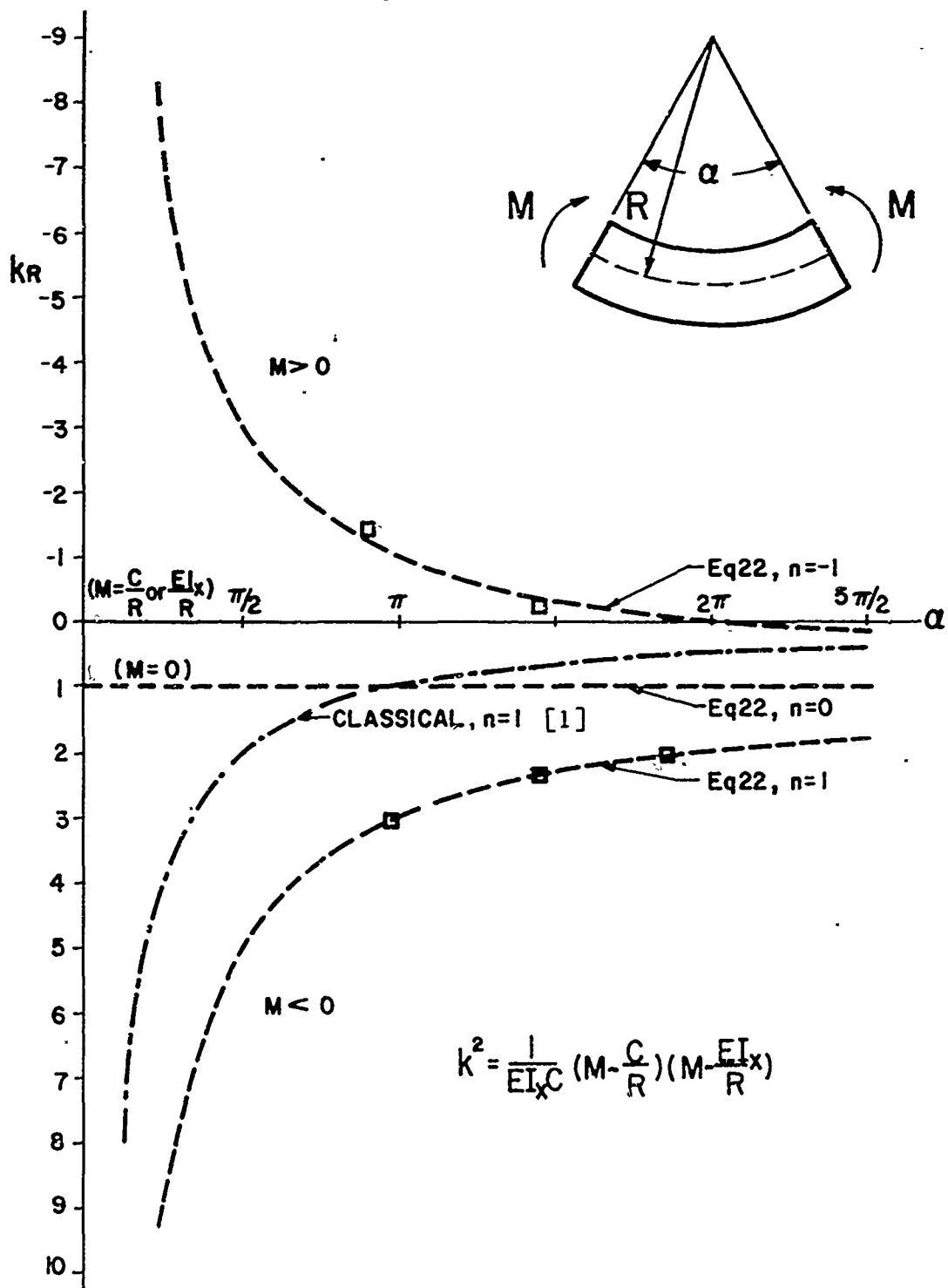


Figure 2. The three lowest eigenvalues of equation (3) vs. beam angle α .

equation (22) vs. beam angle α . For comparison purposes one of the classical curves from equation (6) or (7) is also included. The ordinate of this graph is shown positive downwards in order to emphasize that values of kR less than 1 correspond to a positive (closing) moment and values of kR greater than 1 to a negative (opening) moment.* It can be seen that the classical curve causes the moment to change sign and is asymptotic to a positive value, while the new curves are asymptotic to $kR = 1$ which corresponds to zero buckling moment. The small rectangles on this figure refer to experimental results which will be discussed below.

These uniquely determined values of k are next used to determine the value of the buckling moment M from equation (4). However, since equation (4) is quadratic in M , extraneous solutions may be encountered. To guard against these extraneous solutions, we note that the upper curve in Figure 2 should only give rise to positive moments and the lower curve to negative moments. In addition, the magnitude of the buckling moment should monotonically decrease with increasing α . This arises from the fact that a curved beam can buckle into the true buckled shape of a shorter curved beam, with the remaining portion having only a rigid body displacement. This "unbent" portion will not change either the potential energy or the boundary conditions; thus the longer beam

* This behavior would have been reversed had $k = -\frac{1}{R}$ been chosen as the fundamental rigid body rotation.

could buckle at the same buckling moment as the shorter beam.

Applying these considerations to the buckling moments obtained from Figure 2 and equation (4), one obtains a typical buckling moment curve as shown in Figure 3. The discontinuity in the positive buckling moment curve arises from the fact that it is composed of portions of two different curves. The lower curve passes thru zero at $\alpha = \pi$ and increases until it reaches a maximum at $\alpha = 2\pi$. The upper curve would begin increasing for α greater than 2π ; thus the decreasing moment requirement results in a discontinuity at $\alpha = 2\pi$, where the buckling moment decreases from $M = \frac{C}{R}$ to $M = \frac{EI}{R}x$. However, this discontinuity is only of theoretical interest, since any real curved beam must necessarily have α less than 2π by some small amount. In passing, it should be noted that these buckling moment curves are the minimum possible for lateral buckling of a curved beam. The addition of any lateral restraints on the ends of the beam can only serve to increase the buckling moments.

It is perhaps helpful to plot the eigenfunctions given by equation (21) in order to show the types of conditions that result at the ends of the beam. Figure 4 is such a plot for the case of buckling under a negative moment. Various values of α are represented between the limiting cases of $\alpha \rightarrow 0$ and $\alpha \rightarrow 2\pi$. Figures 5 and 6 present the same information for buckling under a positive moment and for a rigid body rotation about a diameter. In these plots it is helpful to remember

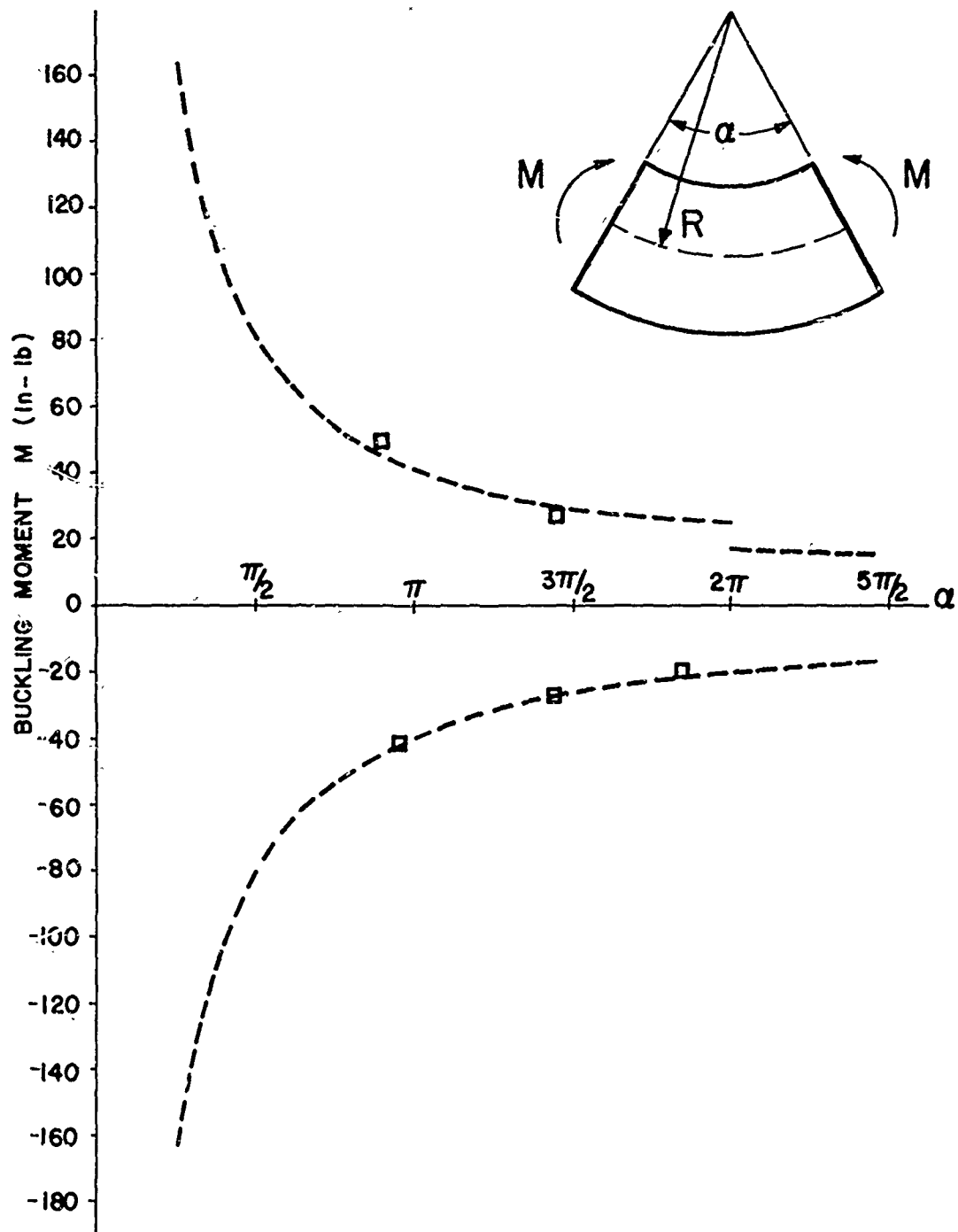


Figure 3. The theoretical buckling moment vs. beam angle α for a curved beam of 5" O.D., $2\frac{1}{2}$ " I.D., and .081" thick, with $E = 5.5 \times 10^5$ psi and $\nu = 0.3$.

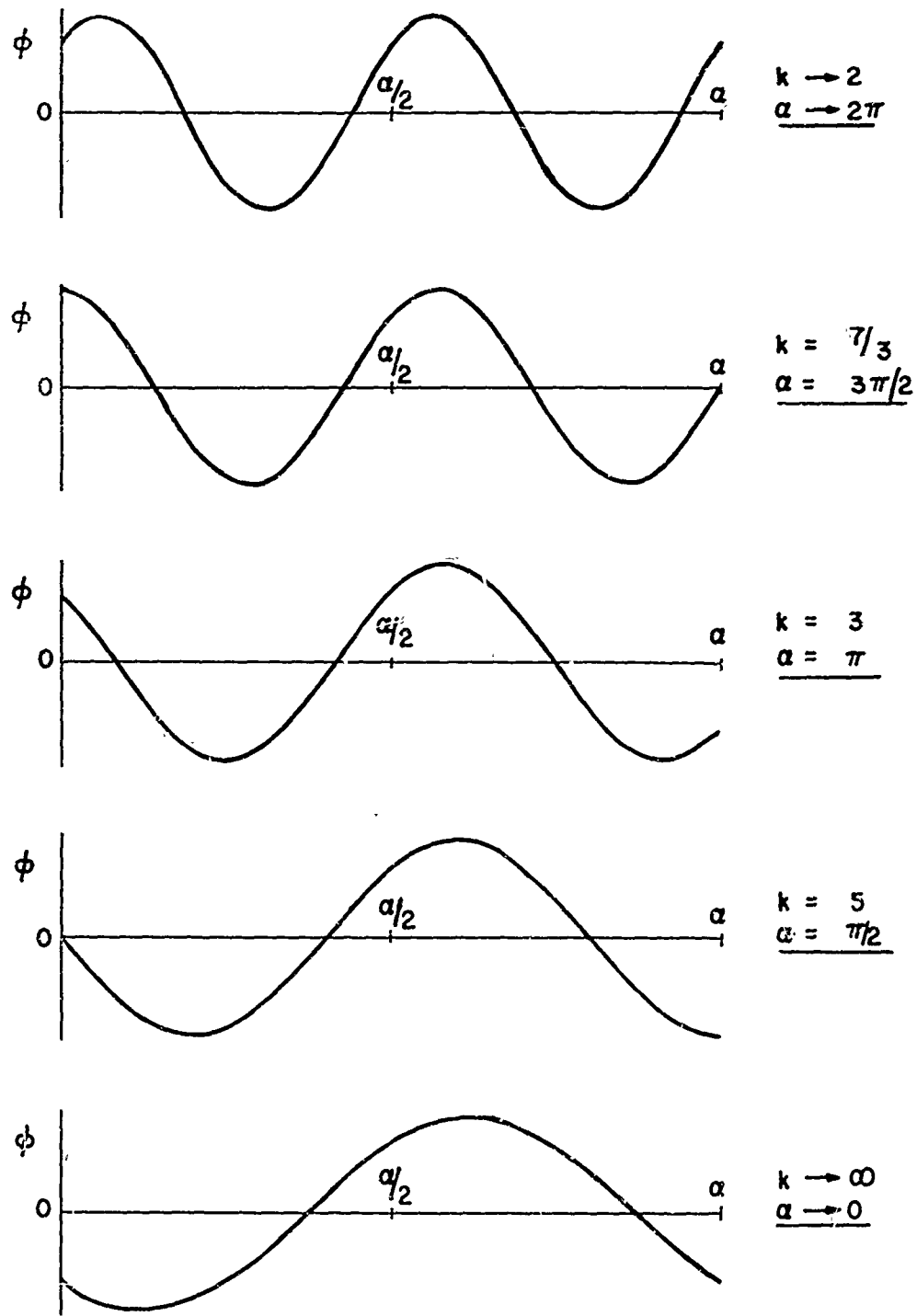


Figure 4. Lowest eigenfunction ϕ_k of equation (3) for buckling under a negative moment (i. e., $n = +1$), for various beam angles α .

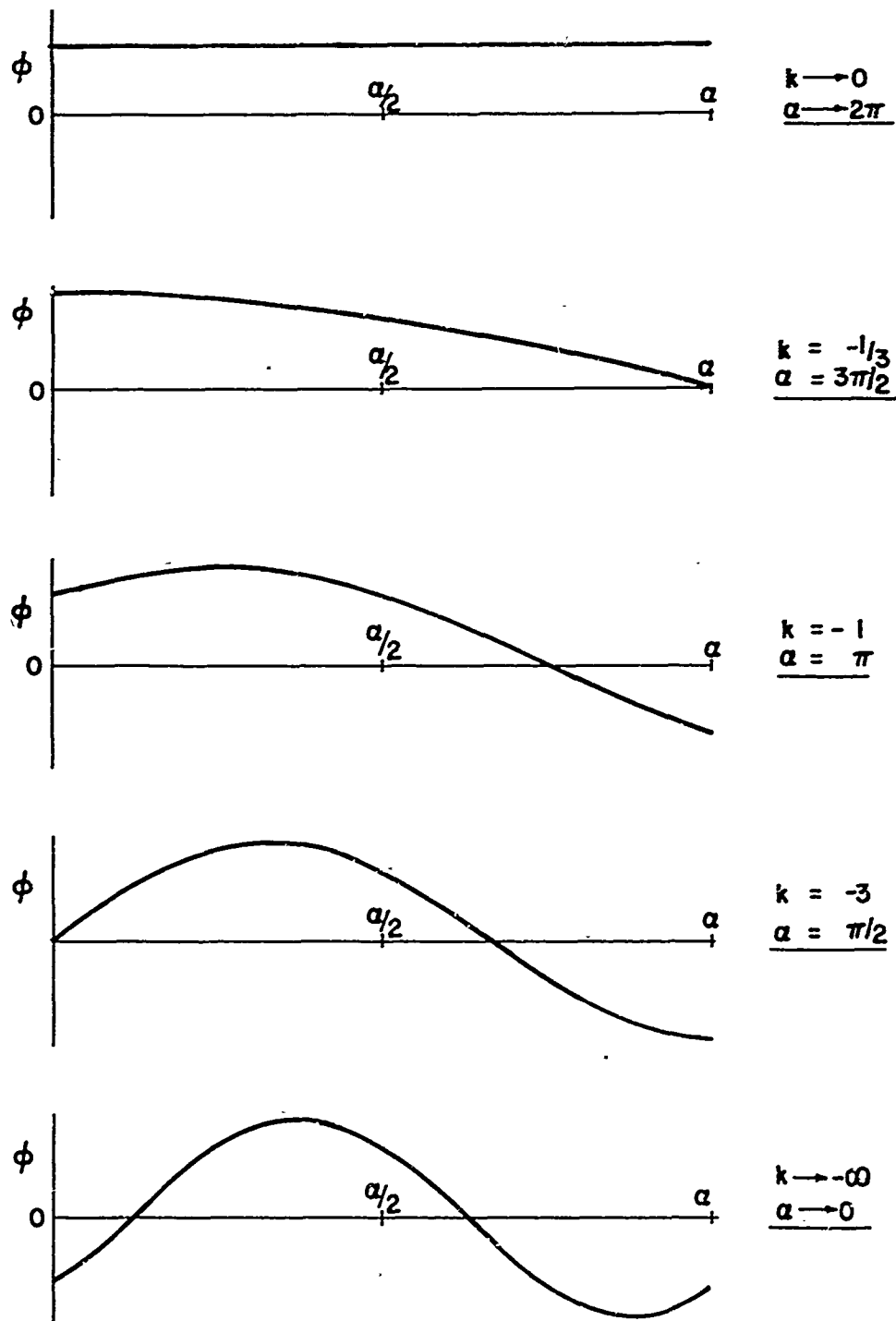


Figure 5. Lowest eigenfunction ϕ_k of equation (3) for buckling under a positive moment (i. e., $n = -1$), for various beam angles α .

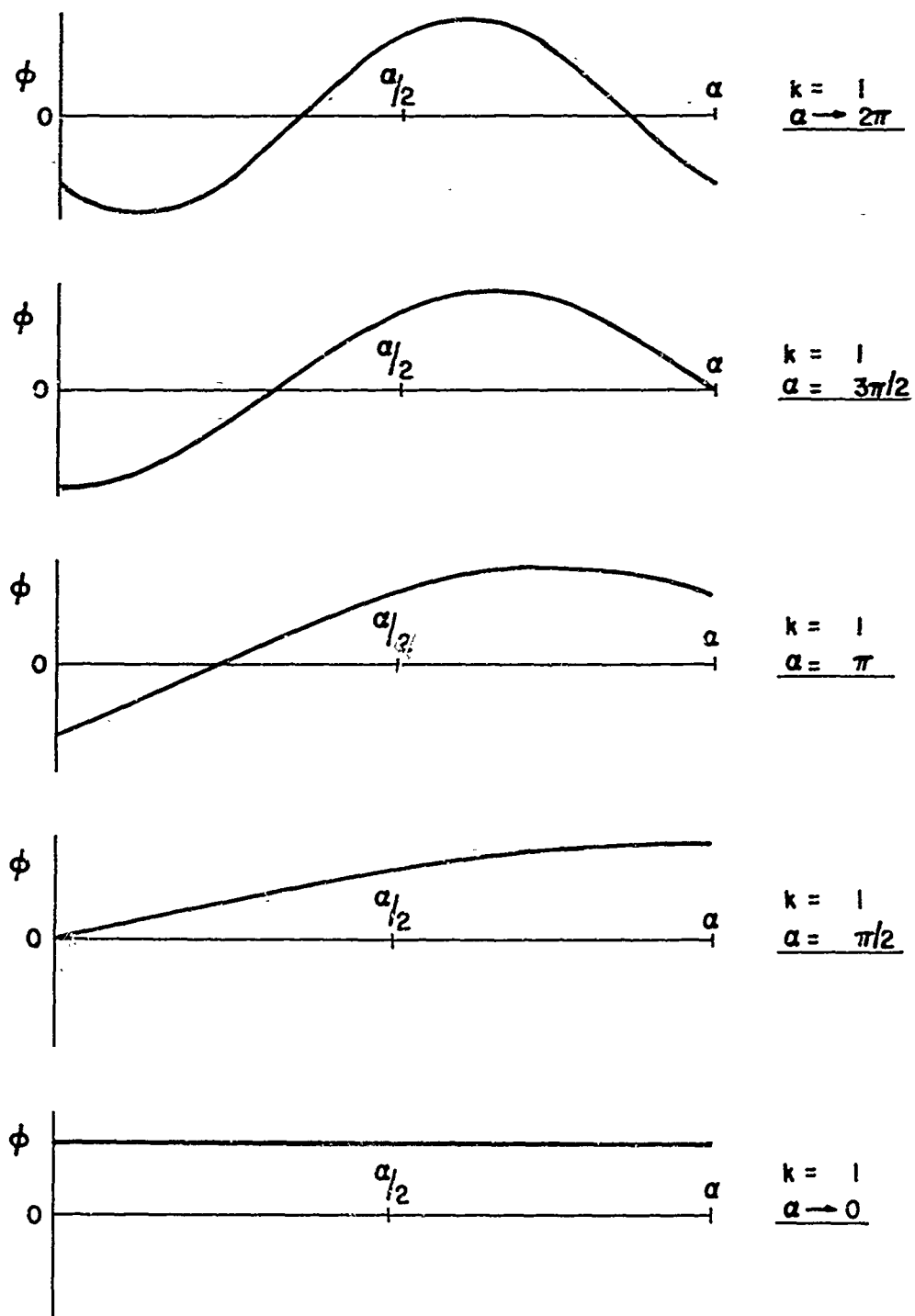


Figure 6. Eigenfunction ϕ_1 of equation (3) for a rigid body rotation about a diameter (i. e., $n = 0$), for various beam angles α .

that k represents the number of full sine waves that would occur if the beam angle were 2π . These curves were obtained by using the plus sign in equation (21); use of the minus sign would essentially interchange the ends. Since φ can be related to v by equations (1) and (2), these curves also represent the deflection of the beam centerline to within an arbitrary rigid body motion. Note that, as would be expected, the eigenfunctions approach the same shape for positive or negative buckling as the beam angle approaches zero. Also, the lowest classical shape, for either positive or negative bending moments, would simply be half of a sine wave regardless of the value of α .

b. Straight beam

One can obtain the buckling moment for a straight beam of length L by taking the limit of the curved beam equation (22) as $R \rightarrow \infty$ and $\alpha R \rightarrow L$. This gives $k = \frac{2n\pi}{L}$ which is twice the accepted classical value [4]. Because of this disagreement, it is necessary to present the analysis although it is similar to that for the curved beam.

The equations for the straight beam can be readily obtained from equations (1) and (2) by omitting those terms which contain $\frac{1}{R}$. In this manner one obtains

$$\frac{d^2\varphi}{ds^2} + k^2\varphi = 0 \quad (23)$$

where

$$k^2 = \frac{M^2}{EI_x C} \quad (24)$$

The solutions to (23) can be written in the form

$$\begin{aligned}\varphi_0 &= A_0 \left(s - \frac{L}{2}\right) + B_0, \\ \varphi_k &= A_k \sin k\left(s - \frac{L}{2}\right) + B_k \cos k\left(s - \frac{L}{2}\right),\end{aligned}\tag{25}$$

where L is the length of the beam. The potential energy V is then derived in the same manner as before and results in

$$V = -\frac{M^2}{2EI} \int_0^L \varphi^2 ds + \frac{C}{2} \int_0^L \left(\frac{d\varphi}{ds}\right)^2 ds.\tag{26}$$

It can be readily seen that the Euler-Lagrange equation of this functional is the equilibrium equation (23). Application of the principle of stationary potential energy again leads to the orthogonality conditions

$$\int_0^L \varphi_k \varphi_l ds = 0,\tag{27}$$

$$\int_0^L \left(\frac{d\varphi_k}{ds}\right) \left(\frac{d\varphi_l}{ds}\right) ds = 0.$$

We note that, for the straight beam, the trivial solution φ_0 is the solution which must be an allowed solution to the problem. Therefore, an application of the orthogonality conditions to the solutions (25) results, after some manipulation, in

$$A_0 A_k \sin \frac{kL}{2} = 0,\tag{28a}$$

$$2A_0 A_k \left(\frac{1}{k} \sin \frac{kL}{2} - \frac{L}{2} \cos \frac{kL}{2}\right) + 2B_0 B_k \sin \frac{kL}{2} = 0,\tag{28b}$$

$$\left(A_{\ell} A_k + B_{\ell} B_k \right) \frac{\sin(k - \ell) \frac{L}{2}}{k - \ell} - \left(A_{\ell} A_k - B_{\ell} B_k \right) \frac{\sin(k + \ell) \frac{L}{2}}{k + \ell} = 0, \quad (28c)$$

$$\left(A_{\ell} A_k + B_{\ell} B_k \right) \frac{\sin(k - \ell) \frac{L}{2}}{k - \ell} + \left(A_{\ell} A_k - B_{\ell} B_k \right) \frac{\sin(k + \ell) \frac{L}{2}}{k + \ell} = 0. \quad (28d)$$

The only solution to the system (28) which has zero potential energy for the trivial solution φ_0 , is

$$\varphi_0 = B_0, \quad (29)$$

$$\varphi_k = A_k \sin k\left(s - \frac{L}{2}\right) + B_k \cos k\left(s - \frac{L}{2}\right)$$

where

$$k = \frac{2n\pi}{L}, \quad n = 0, \pm 1, \pm 2, \dots \quad (30)$$

Note that since the A_k and B_k are arbitrary, equations (29) and (30) contain the limit of equations (21) and (22) (as $R \rightarrow \infty$ and $\alpha R \rightarrow L$) as a special case.

4. EXPERIMENTAL RESULTS

In order to verify the trend of the results given by equations (22) and (30), a short experimental program was undertaken. Since there is a relatively wide disagreement between these results and the classical values, the intent of the experiment was not to provide a rigorous proof of the new results but rather to be of sufficient accuracy to show the disagreement with the classical results.

Before the buckling moment of a curved beam has been reached, the stress distribution is simply that of the well-known plane stress problem of the pure bending of a curved beam [5]. Therefore it was decided to make the test specimens of a photoelastic material in order to have visual proof that the loading was giving the correct theoretical stress distribution before buckling has occurred. The specimens were therefore cut from photoelastic material PS-2B, and were circular ring sectors of 5" O. D., $2\frac{1}{2}$ " I. D., and .081" thick. The specimens were then epoxy bonded to metal strips which were hinged at the center of the circular ring sector. Figure 7 shows an unstressed full ring test specimen in the transmission polariscope with dark field illumination. In this case the metal strip was actually a strap hinge; in other tests it was found necessary to use metal strips bolted to a hinge, so that the center of rotation could be adjusted until the axisymmetric plane stress solution was obtained upon opening or closing the hinge. Figure 8 shows the same specimen after pulling upward on the top of the strap hinge to give a measured opening moment of -16.0 in-lb. It can be seen that the correct axisymmetric stress distribution has been obtained except, of course, in the immediate vicinity of the bonded ends. The first dark fringe is just at the inside radius of the specimen. For this geometry and material, each dark fringe corresponds to a principle stress difference of approximately 970 psi.

Figure 9 shows the same specimen at incipient buckling, and

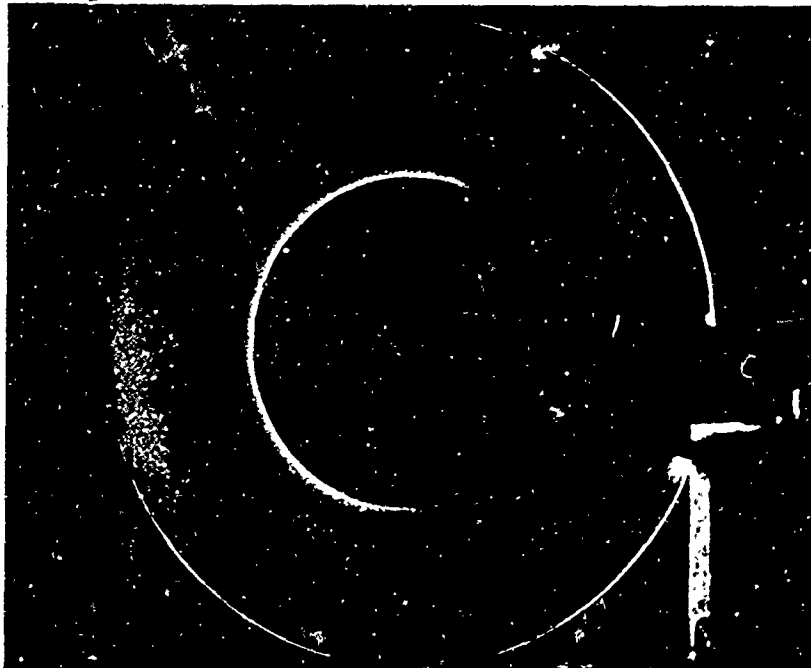


Figure 7. Stress free full ring test specimen in the transmission polariscope with dark field illumination.

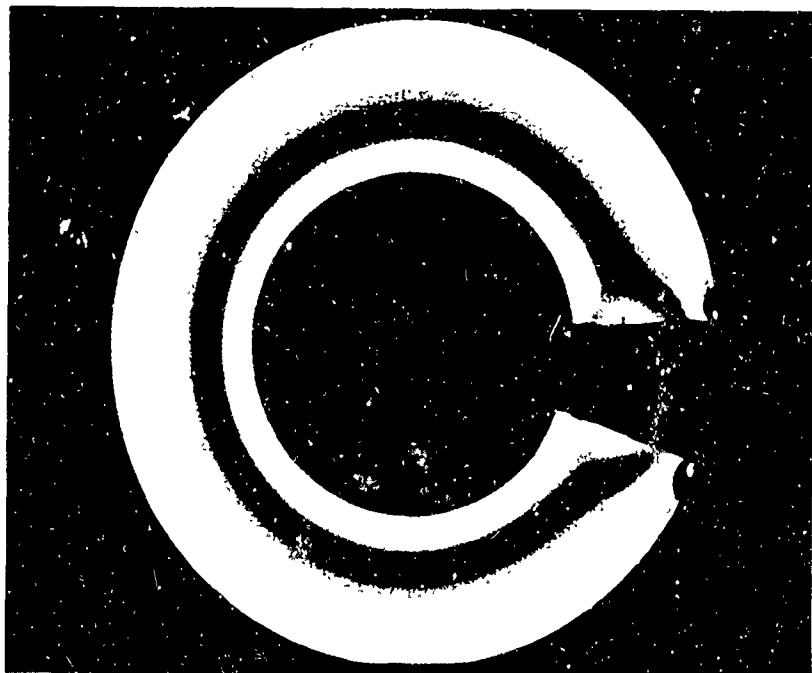


Figure 8. Full ring specimen with an opening moment of -16.0 in-lb. The stress optical coefficient is 970 psi/fringe.

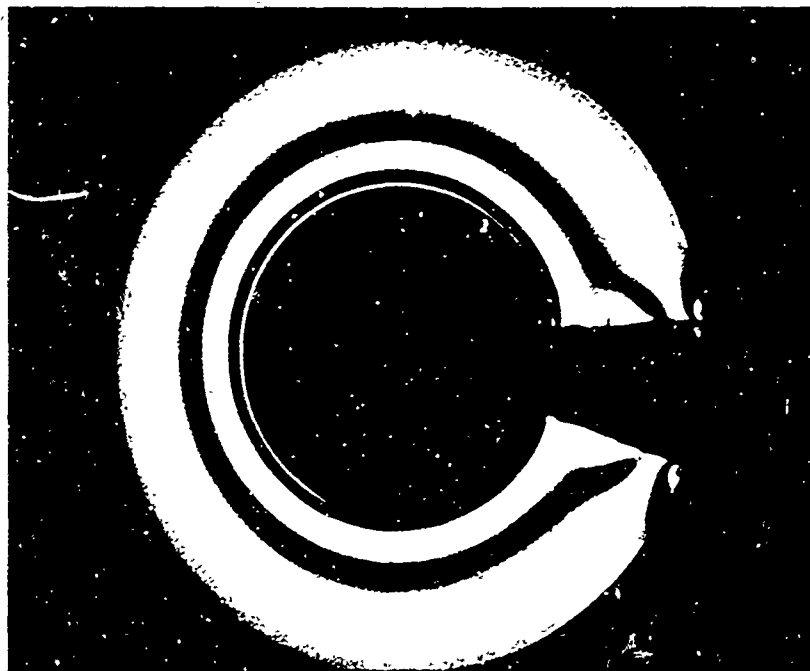


Figure 9. Specimen at incipient buckling with an opening moment of approximately -20.6 in-lb.

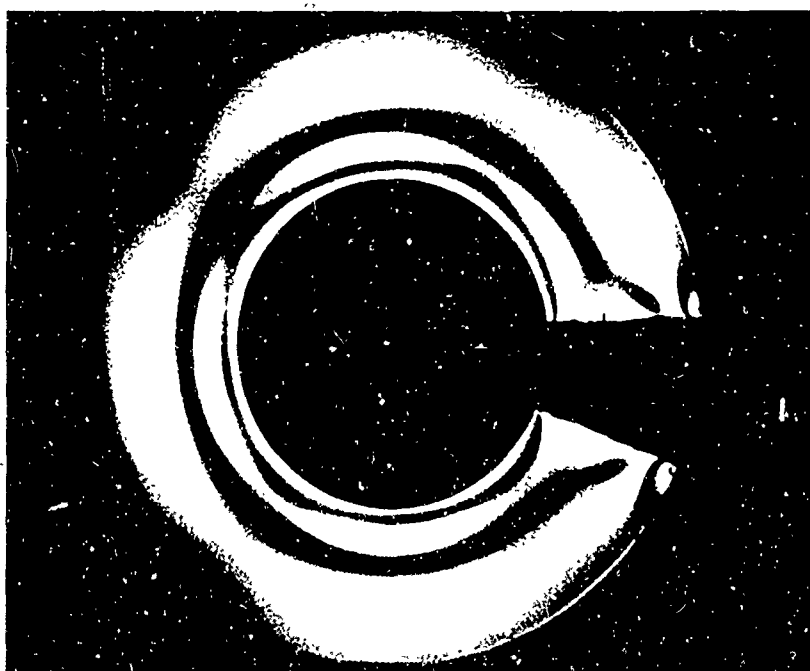


Figure 10. Post-buckled specimen with an opening moment of -20.8 in-lb. The dark radial bands are inflection points.

Figure 10 shows the post-buckled specimen with an opening moment of -20.8 in-lb. The four radial dark bands in Figure 10 were experimentally seen to correspond to the inflection points where $\phi = 0$. This post-buckled shape is, therefore, in fairly good agreement with the topmost theoretical curve shown in Figure 4. Note that the classical post-buckled shape of equation (6) would have no inflection points and the classical shape of equation (7) would have either one or two inflection points, depending on the boundary conditions. The strap hinge arrangement was intended to be loose enough laterally, so that the ends would behave like the "free" edges required by equation (3). However, it is possible that St. Venant's principle applies to this problem, since it was observed that a small deflection of the ends did not seem to contribute to the lateral buckling, in contrast to the problem of buckling under an axial force.

Figures 11 and 12 show the pre- and post-buckled stress distributions for a three-quarter ring specimen which buckled under an opening moment of -27.7 in-lb. The three inflection points in Figure 12 can be seen to be in reasonable agreement with the second theoretical curve of Figure 4. Figures 13 and 14 show the same information for a half ring specimen which buckled at -41.8 in-lb. Some difficulty was encountered in maintaining the plane stress solution for this specimen, and any slight departure from the plane stress solution caused a considerable reduction in the buckling moment. In addition, the lateral restraints had to be maintained so loosely that the buckling process

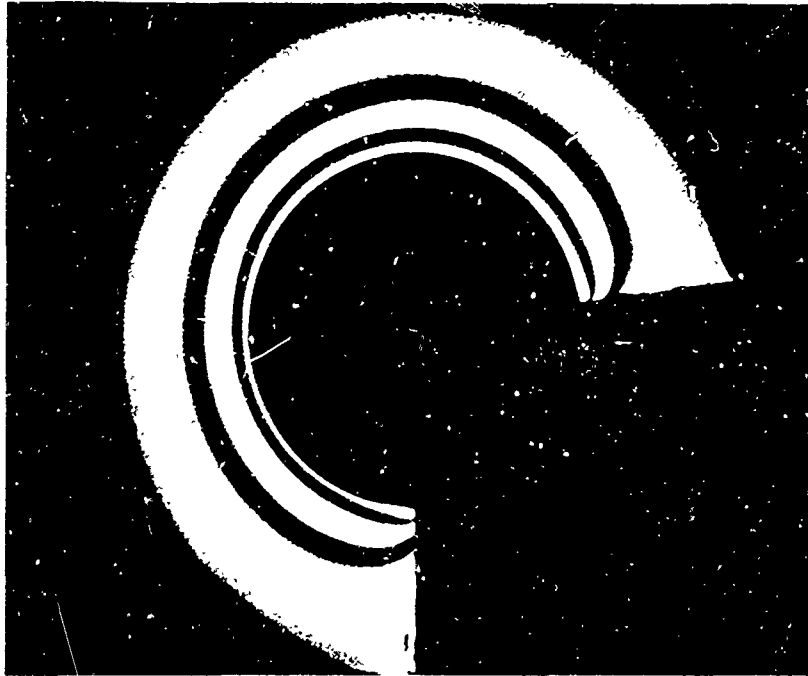


Figure 11. Three-quarter ring specimen with an opening moment of -24.6 in-lb.

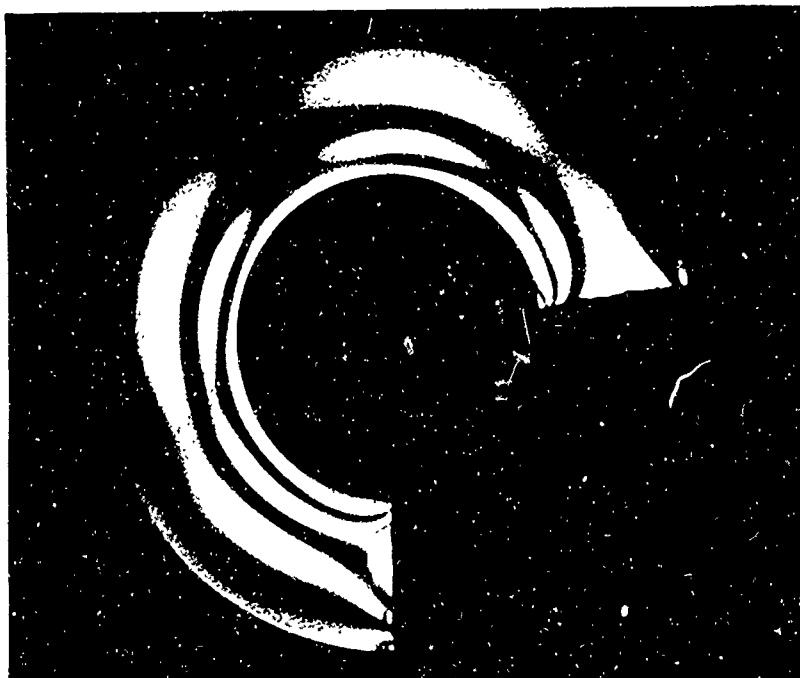


Figure 12. Post-buckled specimen with an opening moment of -28.8 in-lb. The specimen buckled at -27.7 in-lb.

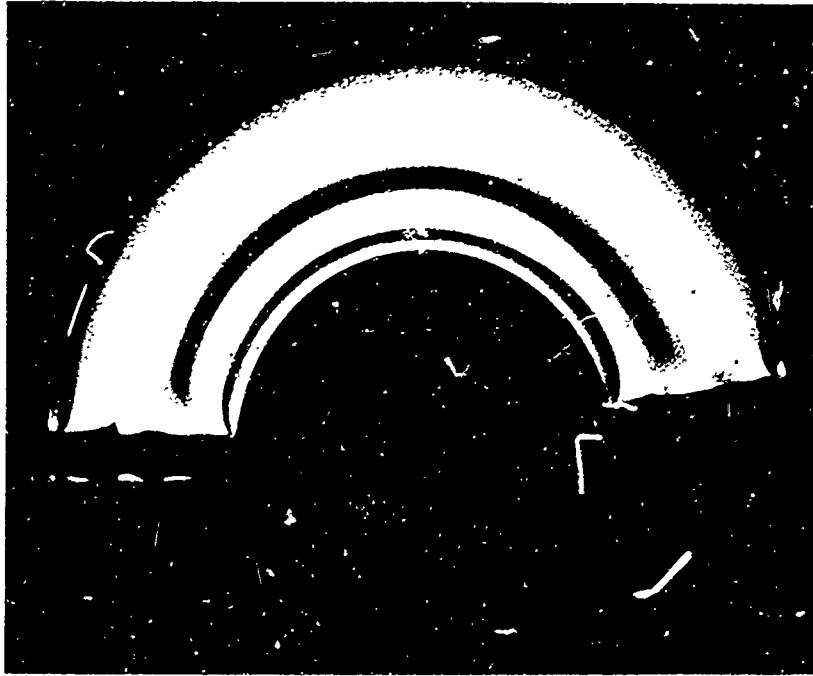


Figure 13. Half ring specimen with an opening moment of -21.9 in-lb.

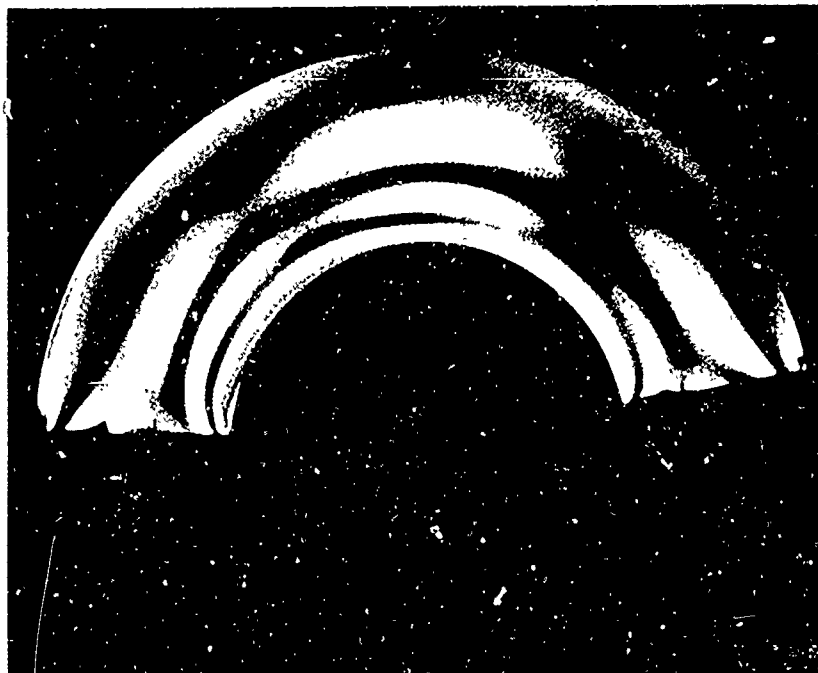


Figure 14. Post-buckled specimen which buckled at an opening moment of -41.8 in-lb.

itself caused a considerable change in the stress distribution. Consequently, the buckled shape in Figure 14 is only in rough agreement with the third theoretical curve of Figure 4.

Data was also obtained for buckling under a closing moment. However, because of a shortage of photoelastic material, the larger specimens were simply cut down to make the shorter specimens; and, due to an unfortunate oversight, no data was obtained on the approximately full ring specimen. The three-quarter ring specimen, however, is shown in Figures 15 and 16 for pre- and post-buckling under a closing moment. The absence of an inflection point is in agreement with the second theoretical curve of Figure 5. Figure 17 shows the half ring specimen with a closing moment of approximately 49 in-lb. A slight increase in this moment appeared to cause the specimen to simultaneously buckle and fracture. Because of this tensile strength limitation, no data on shorter specimens was obtained.

The experimentally obtained buckling moments were used to calculate values of k for these five specimens. These values are indicated by the small squares on Figure 2. In addition, the buckling moments themselves are shown on Figure 3. The amount of agreement between the data points and the theoretical curves should be considered fortuitous, since there were uncertainties in both the experimental procedure and the material properties of the specimens.

Figures 18 and 19 show the pre- and post-buckled stress



Figure 15. Three-quarter ring specimen with a closing moment of +26.0 in-lb.



Figure 16. Post-buckled specimen with a closing moment of +28.0 in-lb.

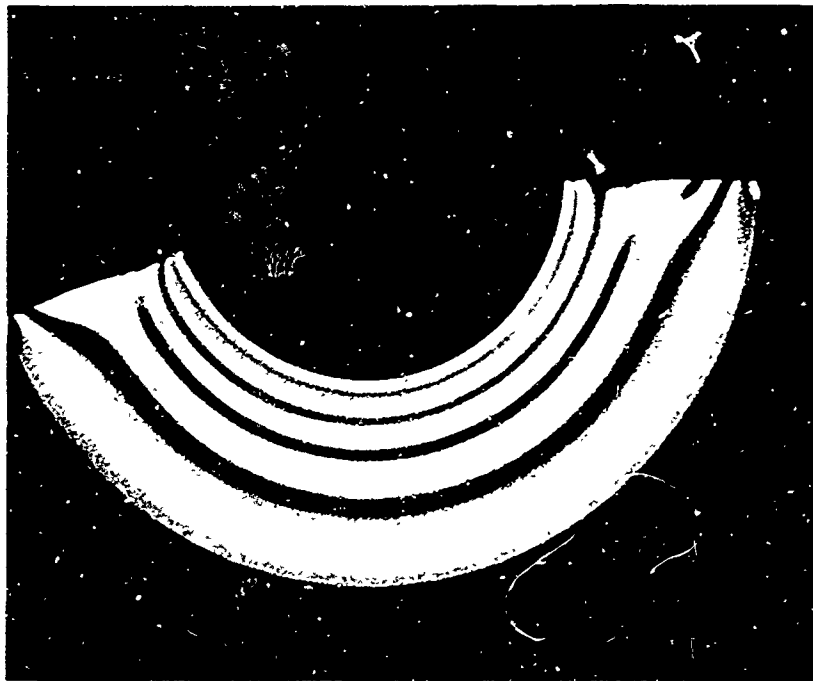


Figure 17. Half ring specimen immediately before failure with a closing moment of +49.0 in-lb.

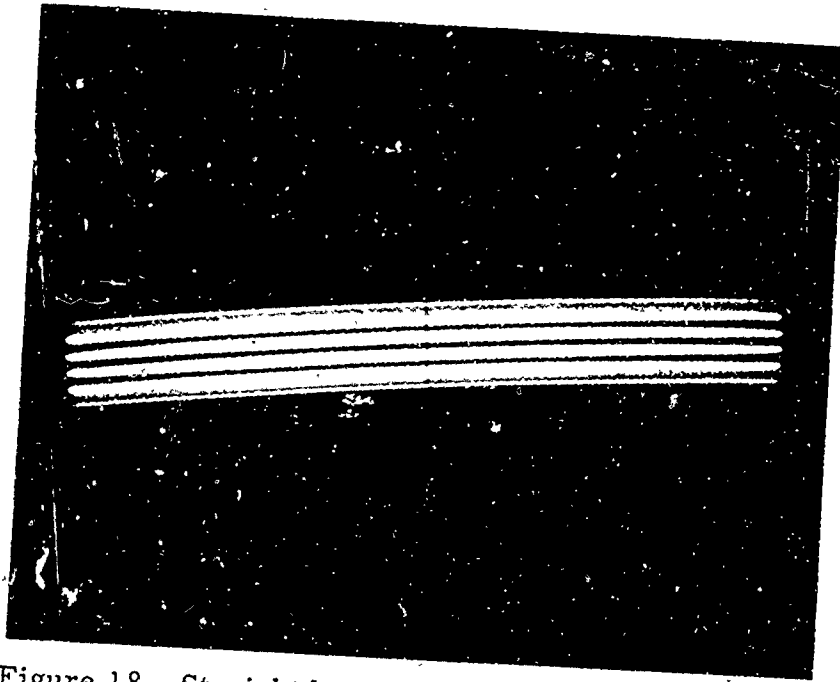


Figure 18. Straight beam specimen with a calculated applied moment of 20.0 in-lb.



Figure 19. Post-buckled specimen.

distributions for an initially straight beam of the same material. The beam dimensions were $7\frac{1}{2}$ " long by 0.8" high and .081" thick. The specimen was epoxy bonded to long transverse metal strips; the right hand strip was clamped to the testing apparatus and the left hand strip remained free. The bending moment was then applied by hand with care being taken to obtain the plane stress solution before buckling had occurred. The applied bending moment was, therefore, calculated from the observed stress pattern, using the dimensions of the beam and the stress optical coefficient of the material.

The specimen remained straight above the classical buckling moment and had a tendency to return to the straight form when a very small buckle was manually introduced. The specimen finally buckled when the calculated applied moment reached a value of 20 in-lb, which is almost exactly twice the lowest classical value for these dimensions; this is in agreement with equation (30). Note the similarity of the buckled shape of Figure 19 to the bottommost theoretical curve of either Figure 4 or Figure 5. This is possibly due to the fact that the straight beam is actually significantly curved before buckling finally occurs.

5. SUMMARY

The basic differential equation for the lateral buckling of a beam subjected to pure bending is derived under the assumption that there are no lateral forces acting on the ends of the beam. Therefore, the classical approach of assigning relatively arbitrary boundary conditions

will, in general, violate this assumption, and there will be shearing forces on the boundaries which were not included in the differential equation. In contrast, the method presented in this paper insures that the principle of stationary potential energy (i. e. , virtual work) is satisfied and the resulting orthogonality conditions lead to a unique set of boundary conditions. The experimental data agrees with these new results rather than the classical results — in magnitude of the buckling moment, as well as in the post-buckled shape of the beam.

APPENDIX

1. Orthogonality Relationships for a Straight Beam Subjected to an Axial Force.

For an initially straight beam subjected to an axial force P whose direction of action remains fixed in space, the equilibrium equation for the deflection v of the beam is

$$EI \frac{d^4 v}{ds^4} + P \frac{d^2 v}{ds^2} = 0 \quad (1)$$

Since the force P is the only agent doing work on the beam, the potential energy expression for the beam, in the case of an inextensible centerline, is given by

$$V = \frac{EI}{2} \int_0^L \left(\frac{d^2 v}{ds^2} \right)^2 ds - \frac{P}{2} \int_0^L \left(\frac{dv}{ds} \right)^2 ds \quad (2)$$

We now consider that we have a complete set of solutions v_k to equation (1) which satisfy the same natural boundary conditions giving rise to (1) and (2); i. e., either the moment or the slope is zero on the boundaries, and, either the shear or the displacement is zero on the boundaries. We now apply the principle of stationary potential energy at the eigenstates v_k and v_l . Taking a varied state about the true state v_k in the form $v^* = v_k + \epsilon v_l$, we obtain from equation (2),

$$\left. \frac{\partial V(v^*)}{\partial \epsilon} \right|_{\epsilon=0} = 0 = \frac{EI}{2} \int_0^L \left(\frac{d^2 v_k}{ds^2} \right) \left(\frac{d^2 v_l}{ds^2} \right) ds - \frac{P}{2} \int_0^L \left(\frac{dv_k}{ds} \right) \left(\frac{dv_l}{ds} \right) ds \quad (3)$$

Taking a varied state about the true state v_l in the form $v^{**} = v_l + \epsilon v_k$,

we obtain

$$\frac{\partial V(v^{**})}{\partial \epsilon} \Big|_{\epsilon \rightarrow 0} = 0 = \frac{EI}{2} \int_0^L \left(\frac{d^2 v_k}{ds^2} \right) \left(\frac{d^2 v_l}{ds^2} \right) ds - \frac{P_l}{2} \int_0^L \left(\frac{dv_k}{ds} \right) \left(\frac{dv_l}{ds} \right) ds. \quad (4)$$

Therefore, if $P_k \neq P_l$, we obtain from equations (3) and (4) the following orthogonality relations for the eigenfunctions:

$$\int_0^L \left(\frac{d^2 v_k}{ds^2} \right) \left(\frac{d^2 v_l}{ds^2} \right) ds = 0, \quad (5)$$

$$\int_0^L \left(\frac{dv_k}{ds} \right) \left(\frac{dv_l}{ds} \right) ds = 0.$$

REFERENCES

1. Timoshenko, S., and J. M. Gere, Theory of Elastic Stability, McGraw-Hill, 2nd ed., 1961, p. 315.
2. Bleich, H. H., Buckling Strength of Metal Structures, McGraw-Hill, 1952, Ch. IV.
3. Love, A. E. H., A Treatise on the Mathematical Theory of Elasticity, Dover Publications, 4th ed., 1944, Ch. XIX.
4. Timoshenko, S., and J. M. Gere, Theory of Elastic Stability, McGraw-Hill, 2nd ed., 1961, p. 257.
5. Timoshenko, S., and J. N. Goodier, Theory of Elasticity, McGraw-Hill, 2nd ed., 1951, p. 61.

Unclassified

Security Classification

DOCUMENT CONTROL DATA - R & D

Security classification of title, body of abstract and indexing annotation must be entered when the overall report is classified

1 ORIGINATING ACTIVITY (Corporate author) UNIVERSITY OF CALIFORNIA, SAN DIEGO La Jolla, California 92037		2a. REPORT SECURITY CLASSIFICATION Unclassified	
		2b. GROUP	
3 REPORT TITLE THE LATERAL BUCKLING OF A STRAIGHT OR CURVED BEAM SUBJECTED TO PURE BENDING			
4 DESCRIPTIVE NOTES (Type of report and inclusive dates) Research Report			
5 AUTHOR(S) (First name, middle initial, last name) F. E. Vanslager			
6 REPORT DATE July 1968	7a. TOTAL NO. OF PAGES 40	7b. NO. OF REFS 5	
8a. CONTRACT OR GRANT NO. N00014-67-A-0109-0003	9a. ORIGINATOR'S REPORT NUMBER(S) No. 21		
b. PROJECT NO. NR 064-496			
c.	9b. OTHER REPORT NO(S) (Any other numbers that may be assigned this report)		
d.			
10 DISTRIBUTION STATEMENT Reproduction in whole or in part is permitted for any purpose of the United States Government. Distribution of this document is unlimited.			
11 SUPPLEMENTARY NOTES		12. SPONSORING MILITARY ACTIVITY Office of Naval Research Washington, D. C.	
13 ABSTRACT <p>This paper presents a new analysis of the classical problem of the lateral buckling under pure bending of a curved beam with circular axis. Although a solution to this problem, and to the corresponding straight beam problem is well-accepted in the literature, the present analysis gives buckling moments which are significantly different than the usually accepted results. The difference arises from an application of new boundary conditions that are shown to be the only boundary conditions consistent with the equilibrium of the buckled beam under a pure bending moment. This new analysis provides generally higher bending moments. A short experimental program was performed, and the results tend to confirm the new analysis.</p>			

DD FORM 1473

Unclassified

Security Classification

Unclassified

Security Classification

14. KEY WORDS	LINK A		LINK B		LINK C	
	ROLE	WT	ROLE	WT	ROLE	WT
Buckling, Lateral buckling of beams, Buckling, experimental, Buckling under pure bending, Curved beam, Elastic stability						

Unclassified

Security Classification